HHS Public Access

Author manuscript

Biol Psychiatry. Author manuscript; available in PMC 2023 March 15.

Published in final edited form as:

Biol Psychiatry. 2022 March 15; 91(6): 561–571. doi:10.1016/j.biopsych.2021.06.024.

Mapping neural circuit biotypes to symptoms and behavioral dimensions of depression and anxiety

Andrea N Goldstein-Piekarski[†,1,2], **Tali M Ball**[†,1], **Zoe Samara**[‡,1], **Brooke R Staveland**[‡,1], **Arielle S. Keller**[‡,1,4], **Scott L Fleming**[‡,1,3], **Katherine A Grisanzio**[‡,1], **Bailey Holt-Gosselin**[1,‡], **Patrick Stetz**[1,2,‡], **Jun Ma**[5,6,‡], **Leanne M Williams**[*,1,2]

[1]Psychiatry and Behavioral Sciences, Stanford University, Stanford, CA, USA

[2]Sierra-Pacific Mental Illness Research, Education, and Clinical Center (MIRECC) Veterans Affairs Palo Alto Health Care System, Palo Alto, CA, USA

[3]Biomedical Informatics, Stanford University, Stanford, CA, USA

[4]Graduate Program in Neurosciences, Stanford University, Stanford, CA, USA

[5]Department of Medicine, University of Illinois at Chicago

[6]Institute for Health Research and Policy, University of Illinois at Chicago

Abstract

Background: Despite tremendous advances in characterizing human neural circuits that govern emotional and cognitive functions impaired in depression and anxiety, we lack a circuit-based taxonomy for depression and anxiety that captures transdiagnostic heterogeneity and informs clinical decision-making.

Methods: We developed and tested a novel system for quantifying six brain circuits reproducibly and at the individual patient level. We implemented standardized circuit definitions relative to a healthy reference sample, and algorithms to generate circuit clinical scores for the overall circuit and its constituent regions.

Results: In new data from primary and generalizability samples of depression and anxiety (n=250), we demonstrate that overall disconnections within task-free salience and default mode

[*]Corresponding author Leanne M. Williams, Department of Psychiatry and Behavioral Sciences, Stanford University School of Medicine, Stanford, CA 94305, USA, Telephone: 650-723-3579, leawilliams@stanford.edu.

[†]These authors contributed equally to this work as first authors

[‡]These authors contributed equally to this work

ARTICLE INFORMATION

LMW designed the study, imaging and conceptualized the image processing system and theoretically motivated analytic approach. ANG-P, TMB, ZS, and LMW implemented the theoretically motivated analytic approach. ANG-P, BRS, and PS with LMW implemented the image processing system. KAG and LMW implemented the phenotype battery and construct analyses for the primary sample. KAG and BHG collected data for the primary and generalizability samples. LMW designed and oversaw the antidepressant treatment study design, JM and LMW designed and oversaw the behavioral intervention treatment study design, and BRS and ASK implemented the treatment analyses and illustration. ANG-P, TMB, ZS, BRS, KAG, SLF, and LMW analyzed data. ANG-P, TMB, ZS, ASK, and LMW wrote the paper. KAG, SLF, BRS, BHG, PS, and JM critically reviewed the paper.

circuits map onto symptoms of anxious avoidance, loss of pleasure, threat dysregulation, and negative emotional biases – core characteristics that transcend diagnoses – and poorer daily function. Regional dysfunctions within task-evoked cognitive control and affective circuits may implicate symptoms of cognitive and valence-congruent emotional functions. Circuit dysfunction scores also distinguish response to antidepressant and behavioral intervention treatments in an independent sample (n=205).

Conclusions: Our findings articulate circuit dimensions that relate to trans-diagnostic symptoms across mood and anxiety disorders. Our novel system offers a foundation for deploying standardized circuit assessments across research groups, trials, and clinics to advance more precise classifications and treatment targets for psychiatry.

Keywords

functional brain circuit imaging; biotype; clinical translation; precision mental health; depression; anxiety

INTRODUCTION

Advances in non-invasive functional brain imaging suggest that distinct types of brain circuit dysfunctions may underlie the clinical expression of depression and anxiety disorders. Yet, we lack a method for quantifying clinical brain circuit metrics in a subject-level manner to facilitate actionable decisions. To make progress toward this goal, we leveraged multiple samples of depression and anxiety to develop and test a subject-level image system suitable for clinical applications.

Our approach was informed by a prior theoretical synthesis of functional brain imaging studies that implicate dysfunction across six large-scale circuits in the clinical features of depression and anxiety and in their treatment (1, 2) (Figure 1). These prior studies have typically focused on case-control designs to understand group average dysfunctions which, arguably, might conflate multiple underlying profiles of subject-level dysfunction. In the prior synthesis we sought to parse types of circuit dysfunction that might contribute to specific clinical features and treatment outcomes. In the task-free state, intrinsic hyper-connectivity of the default mode circuit implicates rumination, while hypo-connectivity may reflect different symptoms and poorer antidepressant outcomes (1, 2). Hypo-connectivity of insula and amygdala within the salience circuit is observed across mood and anxiety disorders, particularly implicating social anxiety, and anxious avoidance (1, 2). When evoked by tasks using threat stimuli, heightened amygdala activation and reduced amygdala-prefrontal connectivity has been observed across disorders, suggesting a common underlying threat-related circuit disruption (1, 2). Within the positive affective circuit, striatal hypo-activation is implicated in reward-related behaviors characteristic of anhedonia (1, 2). Frontoparietal attention circuit hypo-connectivity implicates poor attention symptoms in both depression and anxiety. Under task conditions, frontal hypo-activation within the cognitive control circuit is indicative of more task-specific cognitive symptoms (1, 2).

Informed by our theoretical synthesis (2), we tested the working hypotheses that specific types of circuit clinical function show a one-to-one association with specific clinical

phenotypes (Figure 1). To test these hypotheses, we developed standardized definitions of activation and connectivity for six circuits of interest and a new method for quantifying circuit clinical scores for each circuit for each subject, expressed in standard deviation units from a healthy reference sample. We leveraged multiple samples, spanning healthy subjects, untreated clinical subjects and subjects tested in both pharmacological and behavioral intervention trials, each assessed with common circuit and clinical data elements. These multiple samples afforded us the opportunity to address challenges inherent in developing a subject-level imaging system, including the lack of well-powered samples for which data can be pooled and used to test generalizability. Circuit clinical scores were tested for hypothesized associations with symptom and behavioral phenotypes in untreated samples. Circuit associations with daily function were also explored, relevant to the disabling effects of depression and anxiety (3). To further test the clinical relevance of our system, we evaluated whether circuit clinical scores distinguish intervention response outcomes.

METHODS

Samples

The study comprised four samples assessed with common measures (Tables S1, S2; Methods S2):

- **i.** Healthy reference sample of 95 adults recruited at the same two sites as clinical subjects.
- **ii.** Primary clinical sample of 160 adults with symptoms of depression and anxiety, randomly stratified into subsamples A (70%; n=112) and B (30%; n=48) powered to detect circuit-phenotype associations of small-to-medium size at alpha = 0.05, and control for over-estimated effect sizes (4).
- **iii.** Generalizability sample of 90 adults with clinical characteristics like the primary sample, yet independently recruited.
- **iv.** Treatment sample of 205 adults, enrolled in randomized controlled trials of antidepressant pharmacotherapy for major depressive disorder (n=137) (5, 6) or behavioral intervention for clinically significant depressive symptoms and obesity (n=68) (7), in which treatment response was defined as ≥50% reduction in symptom severity.

Subjects provided written informed consent. Procedures were approved by the Stanford University Institutional Review Board (IRB 27937 and 41837) or Western Sydney Area Health Service Human Research Ethics Committee.

Derivation of Circuits

A consensus definition was generated for circuits of interest using the meta-analytic database Neurosynth.org (8) with search terms “Default Mode, Salience, Attention, Threat, Reward, and Cognitive Control”, and uniformity maps with a false discovery rate (FDR) threshold of .01 (Figure 2A; Methods S3, S4a).

Resulting region pairs were quantified for intrinsic functional connectivity after regressing out task effects (9). Task-evoked activation was quantified for regions of interest, and functional connectivity using psychophysiological interactions between these regions, for the contrasts of sad versus neutral and threat versus neutral faces for negative affect circuit[a], happy versus neutral faces for positive affect circuit, and NoGo versus Go trials for cognitive control circuit (Methods S4c) (Figure 2B).

These regional quantifications were evaluated against quality control and psychometric criteria (Figure 2C). We excluded regions with gray matter overlap of <50%, temporal signal-to-noise ratios (tSNRs) below standard deviation criteria (Methods S4) and regions of intrinsic connectivity with inadequate internal consistency (Figure 2D; Methods S4). The refined set of regions (Figure 2E) were assigned standard anatomical definitions (Tables S3A, B).

Derivation of Circuit Clinical Scores

Subject-level circuit clinical scores were computed for the subset of regions that met quality and psychometric criteria and that are also implicated in our theoretical synthesis of dysfunctions in depression and anxiety (2) (Figure 2F; S4A). In these circuit clinical scores, activation and connectivity were expressed in standard deviation units relative to the healthy reference sample and reference mean of zero (Figure 3, row 2; Methods S5B). Global circuit clinical scores were computed for each subject by averaging component regional scores once the direction of functional connectivity component scores were oriented reflect the hypothesized direction of dysfunction (Figure 3; row 3). Components were weighted evenly given evidence for the reliability of circuit averages (10) and lack of evidence for differential contributions. Internal consistency for global and regional circuit clinical scores was adequate (Figure S5) and global scores were mutually independent, supporting their validity as canonical circuit constructs (Figure S6).

Content and Construct Validation of Clinical Phenotypes

Symptom Phenotypes—To operationalize symptom phenotypes, we followed a content validation procedure (11). Items from scales with broad symptom coverage (Methods S6A; Table S6) were assigned to clinical phenotypes implicated in our theoretical taxonomy (2) and refined by principal component analysis (PCA), yielding six phenotypes labeled ‘rumination’, ‘anxious avoidance’, ‘threat dysfunction’, ‘anhedonia’, ‘negative bias’, and ‘inattention-cognitive dyscontrol’ (Methods S6B; Table S7). Phenotypes were quantified as the average of standardized scores for each subject (Methods S6C).

Behavioral Phenotypes—An equivalent content validation procedure was used to operationalize behavioral phenotypes based on tests assessing general and emotional cognition (Methods S7A) (12). For general cognition, five constructs aligned with a prior PCA conducted during test development (12) - sustained attention (N-Back Continuous Performance Test), response inhibition (Go-NoGo), information processing speed (Stroop and Trails-B), executive function (Maze) and working memory (Digit Span) - and a sixth

[a]Equivalent threat vs neutral contrasts were undertaken for stimuli presented under conscious and nonconscious conditions.

included an interference measure unavailable during test development (Methods S7B; Table S8). For emotional cognition, eight constructs aligned with a prior PCA (12, 13): speed for explicit identification of sad, threat, disgust, and happy expressions; and implicit priming of face recognition biased by these expressions (Methods S7B; Table S9). Phenotypes were computed as the averaged standardized test score for each subject (Methods S7C).

Daily Function—Daily function was assessed by the Satisfaction With Life Scale (14) and Social and Occupational Functioning Assessment Scale (15) (Methods S8, Table S10).

Circuit Clinical Scores and Phenotypes

Hypothesized one-to-one mapping between circuit clinical scores and phenotypes (Figure 1) was tested using regression models with age, sex, and number of censored fMRI volumes included as covariates. Results were evaluated for statistical significance and for clinical meaningfulness, according to effect size and generalizability of effects within confidence limits. We used the Benjamini-Hochberg procedure to control the false discovery rate (16) for each family of global and regional circuit scores (Results S1). FDR-adjusted p-values and m-values for each result in Table 1 are presented in Table S11. Effect sizes were expressed as standardized beta coefficient values, indicating the magnitude of change in phenotype associated with one standard deviation change in the circuit predictor. Following the principle that these effect sizes can be interpreted similarly to correlations (17), <0.2 was considered a weak effect, ≥0.2 and ≤0.5 a moderate effect, and >0.5 a strong effect.

First-order regression models, testing hypothesized global circuit–phenotype associations, were run in primary sample A. In these models, *t*-statistics were compared against the null distribution of *t*-scores derived by 1,000 random permutations (18) and significant effects were i by an FDR-corrected threshold of .05 (Table 1.1; Results S1A). Second-order regression models tested hypothesized regional circuit-phenotype associations and significant effects were defined by an FDR-corrected threshold of 0.1 (Table 1.2; Results S1B). Relationships surviving FDR correction in primary sample A were considered to have generalized if beta effect sizes of sample B and/or generalizability samples fell within the 95% bootstrapped confidence interval for sample A.

Circuit Dysfunctions and Treatment Outcomes

Using logistic regression models, we first tested whether global circuit clinical scores are general predictors of response, over and above pre-treatment symptom severity. Next, we used interaction terms to evaluate global circuit clinical scores as differential predictors of response as a function of type of treatment: Selective Serotonin Reuptake Inhibitors (SSRIs: sertraline, escitalopram) or selective Serotonin-Norepinephrine Reuptake Inhibitor (SNRI: extended-release venlafaxine) for antidepressants, and active behavioral intervention (I-CARE) or usual care (U-CARE) for behavioral intervention. Parallel models were undertaken in hierarchical steps, evaluated by chi-squared tests for each set of global and regional circuit predictors. Significant effects were defined by an FDR-corrected threshold of 0.1 and tendencies at the uncorrected threshold of .05 were considered in supplemental analyses to inform future investigations. Effect sizes for regional predictors that contributed to treatment outcomes were reported.

RESULTS

Circuit Clinical Scores and Phenotypes

An overall observation was that clinical phenotypes were associated with global circuit clinical scores in task-free conditions and with regional scores under task conditions (Table 1, Figure 4).

Default Mode Circuit—Global default mode scores reflective of hyper-connectivity were not associated with rumination as operationalized by our phenotype. However, global default mode hypo-connectivity significantly predicted more severe negative bias and anhedonia at the FDR-adjusted threshold, with low-moderate effect size and consistent across the generalizability sample (Table 1.1; Figure 4).

Lower default mode connectivity specific to the left angular gyrus (AG) and anterior medial Prefrontal Cortex (dmPFC) was associated with more severe rumination (Table 1.2; Figure 5). Although this association did not meet the FDR-adjusted threshold, it replicated with low-moderate effect size across primary samples A and B (Table 1.3).

Salience Circuit—Salience circuit hypo-connectivity significantly predicted more severe symptoms across phenotypes, including anxious avoidance (the hypothesized one-to-one association), negative bias, threat dysregulation, anhedonia, and inattention/cognitive dyscontrol at the FDR-adjusted threshold, consistent across samples (Table 1.1; Figure 4). The hypothesized association of salience circuit hypo-connectivity and anxious avoidance was of low-moderate effect size that was consistent across all samples (Table 1.1).

Greater salience circuit clinical scores were also significantly associated with worse satisfaction with life at the FDR-adjusted threshold, with low-moderate effect size and replicated in the primary sample B (Table 1.3; Results S1c).

When considering regional connections, the association between hypo-connectivity and anxious avoidance was specific to the left anterior insula and left amygdala (Table 1.2; Figure 5). Left-right insula hypo-connectivity was associated with symptoms of negative bias, threat dysregulation, and anhedonia, as well as worse satisfaction with life at the FDR-adjusted threshold (Table 1.3).

Attention Circuit—For the attention circuit, clinical phenotypes were not associated with global circuit clinical scores or regional connectivity.

Negative Affect Circuit—For the negative affect circuit evoked by sad stimuli, hypo-activation of the anterior insula, bilaterally, predicted more severe symptoms of negative bias (Table 1.2; Figure 5). These effects did not meet the adjusted alpha threshold but did meet criteria for a consistent effect size of low-moderate magnitude across primary A, primary B, and generalizability samples. Conversely, there was a tendency for threat-elicited right amygdala hyper-activation to predict accelerated responses to identifying these stimuli at the unadjusted alpha threshold with a weak effect size, consistent across primary samples A and B (Table 1.2; Figure 5).

Positive Affect Circuit—The positive affect circuit probed by happy stimuli global circuit clinical scores was not associated with clinical phenotypes. Lower ventral striatal activation showed a tendency for association with slower responses to identifying happy faces at the uncorrected alpha threshold with low-moderate effect size, generalizable across two samples (Table 1.2, Figure 5).

Cognitive Control Circuit—Lower activation of the dorsal anterior cingulate cortex (dACC) showed a tendency toward association with more severe symptoms of inattention/cognitive dyscontrol at the unadjusted alpha level with low-moderate effect size consistent across primary A and generalizability samples (Table 1.2; Figure 5).

Circuit Clinical Scores and Treatment Outcomes

For pharmacotherapy, we observed regional circuit predictors that were differentially related to SSRI versus SNRI outcomes. Pre-treatment default mode connectivity significantly differentiated response outcomes for SSRIs versus SNRIs (p=0.002; Table S14). SNRI non-responders were distinguished by PCC-angular gyrus hyper-connectivity and SNRI responders by relative hypo-connectivity of these regions, whereas there was a tendency toward an opposing profile of hypo-connectivity in SSRI non-responders and hyper-connectivity in SSRI responders (interaction effect size reflecting the standard deviations increase in the log odds of response versus non-response for SSRI versus SNRI for one standard deviation increase in the predictor = −2.12; Table S17; Figure S8C).

Pre-treatment negative affect circuit scores differentiated responders to SSRIs versus SNRIs (Table S14) when elicited by both conscious and nonconscious threat. SSRI responders showed pre-treatment hyper-connectivity of the left amygdala and dACC, and hypo-connectivity of the right amygdala and dACC for conscious threat. SNRI responders showed hypo-activation of the right amygdala and comparative hyper-connectivity of the left amygdala and subgenual ACC for nonconscious threat (Table S17. Figure S8C).

For the behavioral intervention, pre-treatment attention regional connectivity was a differential predictor of subsequent response to I-CARE versus U-CARE (Table S16). I-CARE responders showed hypo-connectivity between the left anterior inferior parietal lobule and left prefrontal cortex within the attention circuit, compared to responders in U-CARE (Table S17; Figure S8D).

Affect circuit function was also a differential predictor of behavioral intervention outcomes (Table S16). I-CARE responders were distinguished by lower ventromedial PFC activation compared to non-responders, whereas the reverse was observed for U-CARE (Table S17; Figure S10D). Within the negative affect circuit elicited by threat relatively lower left amygdala activity distinguished response to I-CARE but non-response to U-CARE (Table S16, S17; Figure S10D).

DISCUSSION

We developed a reproducible image processing system for quantifying subject-level neural circuit metrics and tested these metrics for their clinical utility in showing relationships

with clinical symptoms, behavior and social-occupational function, and treatment response. Our approach offers one step toward making precision advances in the mental health field, specifically for depressive and anxiety disorders that contribute disproportionately to illness burden and suicide.

Our image processing system integrates four key features: standardization, quality-controlled neuroanatomical definitions of functional brain circuits spanning task-free and task-evoked contexts, reproducible procedures for quantifying the activation of and connectivity between regions within each circuit with demonstrated consistency, and algorithms for computing metrics that quantify global and regional circuit clinical scores at the individual subject-level relative to a healthy reference sample. We tested this system in three samples of adults with a broad range of depression and anxiety symptoms, and systematically examined brain circuit-phenotype relations informed by our theoretical framework (2). We found limited evidence for the hypothesized one-to-one mappings between circuit clinical scores and specific phenotypes that reflect common assumptions in the field about neural-phenotype relationships. However, we did identify associations that suggest specific connectivity profiles – particularly within salience and default mode circuits – may give rise to multiple phenotype expressions, and that additional circuit activation and connectivity profiles are implicated in treatment response.

Within the task-free circuits, salience circuit clinical scores, especially hypo-connectivity between the anterior insula and the amygdala, was significantly predictive of anxious avoidance symptoms at the adjusted alpha level, and generalized across samples, consistent with hypotheses (2). Salience circuit hypo-connectivity within the insula also contributed significantly to symptoms of anhedonia, negative bias, and threat dysregulation, and generalized across at least one additional sample. These findings suggest a role for insula disconnection in features of negative bias and blunted positive emotion that impact daily function, consistent with findings from metabolic insula imaging (19). Global salience hypo-connectivity showed an additional significant association with inattention/cognitive dyscontrol symptoms that generalized across samples. Given prior evidence of functional interactions between salience and attention circuits (20) that may fluctuate with interoceptive and external events, future investigations that expand our current within-circuit focus to examine between-circuit connectivity are warranted.

Although default mode *hyper*-connectivity was not predictive of rumination as hypothesized, global *hypo*-connectivity was significantly associated with negative bias and anhedonia at the adjusted alpha level. Such hypo-connectivity is consistent with emerging evidence for a default mode hypo-connectivity subtype of depression (21, 22) and the exploratory default mode biotype proposed in our theoretical framework (1, 2), informed by meta-analysis (23). We also note that our phenotype of rumination indexed ruminative worry in particular; future investigations with broader measures of ruminative response styles are required.

Regarding pharmacological treatment, we found that pre-treatment hyper-connectivity of the posterior cingulate and angular gyrus within the default mode circuit distinguished non-responders from responders to the SNRI in particular. This observation of hyper-connectivity accords with prior findings for dulexotine, which also inhibits both serotonin

and norepinephrine uptake and has been found to regularize pre-treatment default mode hyper-connectivity (24). It also extends upon prior posterior cingulate seed-based and whole-brain connectivity analyses of this dataset that implicate relatively intact default mode connectivity as a general predictor of antidepressant remission (25, 26). Further, SNRI responders were characterized by pre-treatment amygdala hypo-activation within the negative affect circuit, consistent with prior group-averaged findings in this dataset (27). The new finding that SNRI responders are distinguished by amygdala-subgenual anterior cingulate (ACC) hypo-connectivity for nonconscious threat, and SSRI responders by an opposing profile of amygdala-dorsal ACC hyper-connectivity for conscious threat, suggests that amygdala-ACC connectivity might reflect different functional states that are present prior to treatment and that respond to the different ways that the drug types act at the receptor level.

For behavioral intervention, pre-treatment global hypo-connectivity within the attention circuit was a significant differential predictor of response to the active I-CARE condition, consistent with independent reports that such hypo-connectivity could inform selection for cognitive behavior therapy (28). Differential response to behavioral intervention was also distinguished by regional activation elicited by positive and negative affective stimuli. Although these treatment outcome relationships need to be confirmed in independent samples, they offer a starting point for personalized biomarker trials that require a standardized procedure for quantifying circuit dysfunction at the subject-level.

By focusing first on a discrete within-circuit, one-to-one mapping approach, our goal was to develop and evaluate a prototype for subject-level fMRI quantification suited to clinical applications. Taken together, our findings reveal minimal support for a model in which there is a discrete one-to-one mapping between the six circuits of interest and specific symptoms and behaviors implicated in dysfunction of these circuits, at least within the current samples and as based on our prior theoretical synthesis (1, 2). Yet, the findings do demonstrate the reproducibility of the method, and reveal significant and consistent effects for a specific subset of circuit-phenotype associations across samples and for circuit markers of treatment outcomes. Because our circuit clinical scores were validated in samples recruited to be representative of the community, with a range of symptom severity and comorbidities, the method arguably is applicable to the range of patients seen in the clinic (29).

Both the null findings and non-hypothesized associations revealed by analyses, prompt the consideration of limitations, potential alternative explanations, and new directions for future investigation. A crucial consideration in determining circuit-phenotype outputs is the selection of inputs and samples for analysis. Although our recruitment approach achieved representative samples, the inclusion of mildly symptomatic subjects could have limited the opportunity to pinpoint circuit dysfunctions that manifest primarily in severely symptomatic phenotypes that are the focus of case: control designs. Future investigations, currently underway, focus on a strategy of enriching samples based on clinically relevant standard deviation thresholds for both circuit and clinical measures. Relatedly, although our samples spanned multiple diagnostic comorbidities, the most common diagnosis was generalized anxiety disorder, and MDD was three times more prevalent in the generalizability than in the primary sample. The preponderance of anxiety disorders in our sample may have

contributed to the robust results for insula connectivity, in concert with the amygdala. This speculation accords with evidence that the insula, and the salience network it defines, serves a domain-general function that when disrupted can produce the diverse visceral, affective and cognitive features of anxiety (30). Future investigations might determine if these connections are disrupted during tasks that engage threat and other aspects of affective reactivity.

Our clinical inputs were items from well-established symptom scales for which the focus is usually on total scores. Thus, one research product developed from this study is the classification of individual items, across these scales, according to clinical phenotypes suggested by our theoretical circuit taxonomy (1, 2). This classification was validated in the current sample, but we do acknowledge that limited item coverage for some phenotypes may have limited the capacity to identify robust associations with all circuits of interest. For example, the established scales we used lack coverage of ruminative response styles, threat dysregulation, inattention, and cognitive impairments, implicated by respective dysfunctions in the default mode, negative affect, attention, and cognitive control circuits. In ongoing analyses, we pursue symptom-specific scales, to further understand how symptom profiles are identified in the brain.

At the circuit level, it would likewise be important to expand our use of established tasks to include tasks designed to probe more specific circuit constructs, such as fMRI reward tasks. Future investigations are also warranted to expand our initial focus on a specific set of regions informed by prior knowledge (2) to additional regions informed by ongoing evidence. As regional inputs are added, the weighting of these inputs to the computation of global circuit clinical scores may also need refinement and we designed our circuit system to be flexible with the expectation of such refinement. To explore circuit-phenotype associations more fully it will be essential to extend our within-circuit approach to the testing of putative biotypes that include sub-nodes, between-circuit effects, and interactions within and between circuits (1, 2). For example, parsing of sub-nodes of the default mode circuit and their connectivity with negative affect circuits may allow for a better understanding of associations with ruminations, self-reflection and negative attributional biases (2, 31), and accounting for interactions between default mode, attention and cognitive control circuits may provide a more complete characterization of a cognitive dyscontrol biotype (32). Methodologically, it would be valuable to pursue direct tests of the impact of scanner, site, and functional localizers for more precise subject-level quantification (33) and to incorporate finer-grained age norms for more precise interpretation.

Our findings for treatment accord with the view that mechanistic circuit markers for clinical phenotypes may not be the same as those circuit markers that predict treatment outcomes, help select among multiple treatment options, and/or change with treatment (29). Precision medicine, prospective and repeat testing designs are needed to systematically help sort circuit dysfunctions according to these different clinical functions. Such designs will also allow for more precise characterization of which aspects of circuit dysfunction are more trait-like versus state-like and thus which are more amenable to change with treatment.

Conclusion

The functional image system developed and tested in this study offers one means by which our field can generate standardized subject-level imaging metrics across studies, sites, and samples. These metrics can serve as inputs into further subgroup classifications, computational models, and biomarker trials, to refine our understanding of the clinical function of these metrics. Clinically, such metrics offer a step toward the use of imaging tools to aid in the personalized clnical management of mood and anxiety.

Supplementary Material

Refer to Web version on PubMed Central for supplementary material.

ACKNOWLEDGEMENTS AND DISCLOSURES

This work was supported by the National Institutes of Health [grant numbers R01MH101496 (LMW; NCT02220309), UH2HL132368 (JM, LMW; NCT02246413), F32MH108299 (ANG-P), T32MH019938 (TMB), and K23MH113708 (TMB)]. Psychopharmacology data from iSPOT-D (NCT00693849) was sponsored by Brain Resource Ltd.

We acknowledge the contributions of Sarah Chang, BSc, to data acquisition and generating of sample tables and Carlos Correa, BCompSc, to software development of the image processing system. We acknowledge the editorial support of Jon Kilner, MS, MA (Pittsburgh, PA, USA).

The funders had no role in study design, data collection, data analysis, data interpretation, or writing of the report. The corresponding author had full access to all the data in the study and had final responsibility for the decision to submit for publication.

The datasets for the primary sample analyzed during the current study are made available through the National Institutes of Health Database, NDA, https://nda.nih.gov/user/dashboard/collections.html, collection number C2100. The datasets for the generalizability sample analyzed during the current study will be made available from the corresponding author on reasonable request. Patients' whole-brain correlation matrices and our full analysis codes for the primary and generalizability samples are available from the corresponding author on reasonable request. The datasets for the treatments sample analyzed during the current study will be made available from the corresponding author on reasonable request after approval of a proposal. For the antidepressant data, reasonable requests will also require the permission of the study sponsor, Brain Resource Ltd. For the behavioral intervention data, study measures will be made available through the National Institutes of Health Science of Behavioral Change repository, https://scienceofbehaviorchange.org/measures/.

LMW declares US Pants. App. 10/034,645 and 15/820,338: Systems and methods for detecting complex networks in MRI image data. SLF declares consulting fees received from Youper, Inc within the last five years. All other authors report no biomedical financial interests or potential conflicts of interest.

Funding:

This work was supported by the National Institutes of Health [grant numbers R01MH101496 (LMW), UH2HL132368 (JM, LMW), F32MH108299 (ANG-P), T32MH019938 (TMB), and K23MH113708 (TMB)].

REFERENCES

1. Williams LM (2017): Defining biotypes for depression and anxiety based on large-scale circuit dysfunction: a theoretical review of the evidence and future directions for clinical translation. Depress Anxiety. 34:9–24. [PubMed: 27653321]
2. Williams LM (2016): Precision psychiatry: A neural circuit taxonomy for depression and anxiety. The Lancet Psychiatry, pp 472–480. [PubMed: 27150382]
3. Friedrich MJ (2017): Depression Is the Leading Cause of Disability Around the World. JAMA. 317:1517.

4. Button KS, Ioannidis JP, Mokrysz C, Nosek BA, Flint J, Robinson ES, et al. (2013): Power failure: why small sample size undermines the reliability of neuroscience. Nat Rev Neurosci. 14:365–376. [PubMed: 23571845]
5. Grieve SM, Korgaonkar MS, Etkin A, Harris A, Koslow SH, Wisniewski S, et al. (2013): Brain imaging predictors and the international study to predict optimized treatment for depression: study protocol for a randomized controlled trial. Trials. 14:224. [PubMed: 23866851]
6. Williams LM, Rush AJ, Koslow SH, Wisniewski SR, Cooper NJ, Nemeroff CB, et al. (2011): International Study to Predict Optimized Treatment for Depression (iSPOT-D), a randomized clinical trial: rationale and protocol. Trials. 12:4. [PubMed: 21208417]
7. Williams LM, Pines A, Goldstein-Piekarski AN, Rosas LG, Kullar M, Sacchet MD, et al. (2018): The ENGAGE study: Integrating neuroimaging, virtual reality and smartphone sensing to understand self-regulation for managing depression and obesity in a precision medicine model. Behav Res Ther. 101:58–70. [PubMed: 29074231]
8. Yarkoni T, Poldrack R, Nichols T, Van Essen D, Wager T (2011): NeuroSynth: a new platform for large-scale automated synthesis of human functional neuroimaging data. Frontiers in Neuroinformatics Conference Abstract: 4th INCF Congress of Neuroinformatics, pp doi:10.3389/conf.fninf.2011.3308.00058.
9. Korgaonkar MS, Ram K, Williams LM, Gatt JM, Grieve SM (2014): Establishing the resting state default mode network derived from functional magnetic resonance imaging tasks as an endophenotype: A twins study. Human Brain Mapping. 35:3893–3902. [PubMed: 24453120]
10. Ball TM, Goldstein-Piekarski AN, Gatt JM, Williams LM (2017): Quantifying person-level brain network functioning to facilitate clinical translation. Transl Psychiatry. 7:e1248. [PubMed: 29039851]
11. Boateng GO, Neilands TB, Frongillo EA, Melgar-Quinonez HR, Young SL (2018): Best Practices for Developing and Validating Scales for Health, Social, and Behavioral Research: A Primer. Front Public Health. 6:149. [PubMed: 29942800]
12. Mathersul D, Palmer DM, Gur RC, Gur RE, Cooper N, Gordon E, et al. (2009): Explicit identification and implicit recognition of facial emotions: II. Core domains and relationships with general cognition. Journal of Clinical and Experimental Neuropsychology. 31:278–291. [PubMed: 18720178]
13. Williams LM, Mathersul D, Palmer DM, Gur RC, Gur RE, Gordon E (2009): Explicit identification and implicit recognition of facial emotions: I. Age effects in males and females across 10 decades. J Clin Exp Neuropsychol. 31:257–277. [PubMed: 18720177]
14. Diener E, Emmons RA, Larsen RJ, Griffin S (1985): The Satisfaction With Life Scale. J Pers Assess. 49:71–75. [PubMed: 16367493]
15. Morosini PL, Magliano L, Brambilla L, Ugolini S, Pioli R (2000): Development, reliability and acceptability of a new version of the DSM-IV Social and Occupational Functioning Assessment Scale (SOFAS) to assess routine social functioning. Acta Psychiatr Scand. 101:323–329. [PubMed: 10782554]
16. Benjamini YH YB (1995): Controlling the false discovery rate: A practical and powerful approach to multiple testing. J R Stat Soc Ser. 57:289–300
17. Acock AC (2014): A Gentle Introduction to Stata., 4th. ed. Texas: Stata Press.
18. Phipson B, Smyth GK (2010): Permutation P-values should never be zero: Calculating exact P-values when permutations are randomly drawn. Statistical Applications in Genetics and Molecular Biology. 9.
19. Dunlop BW, Kelley ME, McGrath CL, Craighead WE, Mayberg HS (2015): Preliminary Findings Supporting Insula Metabolic Activity as a Predictor of Outcome to Psychotherapy and Medication Treatments for Depression. J Neuropsychiatry Clin Neurosci. 27:237–239. [PubMed: 26067435]
20. Kaiser RH, Andrews-Hanna JR, Wager TD, Pizzagalli DA (2015): Large-Scale Network Dysfunction in Major Depressive Disorder: A Meta-analysis of Resting-State Functional Connectivity. JAMA Psychiatry. 72:603–611. [PubMed: 25785575]
21. Yan CG, Chen X, Li L, Castellanos FX, Bai TJ, Bo QJ, et al. (2019): Reduced default mode network functional connectivity in patients with recurrent major depressive disorder. Proc Natl Acad Sci U S A. 116:9078–9083. [PubMed: 30979801]

22. Tozzi L, Zhang X, Chesnut M, Holt-Gosselin B, Ramirez CA, Williams LM (2021): Reduced functional connectivity of default mode network subsystems in depression: Meta-analytic evidence and relationship with trait rumination. Neuroimage Clin. 30:102570. [PubMed: 33540370]

23. Zhu X, Wang X, Xiao J, Liao J, Zhong M, Wang W, et al. (2012): Evidence of a dissociation pattern in resting-state default mode network connectivity in first-episode, treatment-naive major depression patients. Biol Psychiatry. 71:611–617. [PubMed: 22177602]

24. Posner J, Hellerstein DJ, Gat I, Mechling A, Klahr K, Wang Z, et al. (2013): Antidepressants normalize the default mode network in patients with dysthymia. JAMA Psychiatry. 70:373–382. [PubMed: 23389382]

25. Korgaonkar MS, Goldstein-Piekarski AN, Fornito A, Williams LM (2020): Intrinsic connectomes are a predictive biomarker of remission in major depressive disorder. Mol Psychiatry. 25:1537–1549. [PubMed: 31695168]

26. Goldstein-Piekarski AN, Staveland BR, Ball TM, Yesavage J, Korgaonkar MS, Williams LM (2018): Intrinsic functional connectivity predicts remission on antidepressants: a randomized controlled trial to identify clinically applicable imaging biomarkers. Transl Psychiatry. 8:57. [PubMed: 29507282]

27. Williams LM, Korgaonkar MS, Song YC, Paton R, Eagles S, Goldstein-Piekarski A, et al. (2015): Amygdala Reactivity to Emotional Faces in the Prediction of General and Medication-Specific Responses to Antidepressant Treatment in the Randomized iSPOT-D Trial. Neuropsychopharmacology. 40:2398–2408. [PubMed: 25824424]

28. Yang Z, Gu S, Honnorat N, Linn KA, Shinohara RT, Aselcioglu I, et al. (2018): Network changes associated with transdiagnostic depressive symptom improvement following cognitive behavioral therapy in MDD and PTSD. Mol Psychiatry. 23:2314–2323. [PubMed: 30104727]

29. Rush AJ, Ibrahim HM (2018): A Clinician's Perspective on Biomarkers. Focus (Am Psychiatr Publ). 16:124–134. [PubMed: 31975907]

30. Paulus MP, Stein MB (2006): An insular view of anxiety. Biol Psychiatry. 60:383–387. [PubMed: 16780813]

31. Zhou HX, Chen X, Shen YQ, Li L, Chen NX, Zhu ZC, et al. (2020): Rumination and the default mode network: Meta-analysis of brain imaging studies and implications for depression. Neuroimage. 206:116287. [PubMed: 31655111]

32. Williams LM, Coman JT, Stetz PC, Walker NC, Kozel FA, George MS, et al. (2021): Identifying response and predictive biomarkers for Transcranial magnetic stimulation outcomes: protocol and rationale for a mechanistic study of functional neuroimaging and behavioral biomarkers in veterans with Pharmacoresistant depression. BMC Psychiatry. 21:35. [PubMed: 33435926]

33. Mehraveh Salehi ASG, Karbasi Amin, Shen Xilin, Scheinost Dustin, Todd Constable R (2018): There is no single functional atlas even for a single individual: Parcellation of the human brain is state dependent.

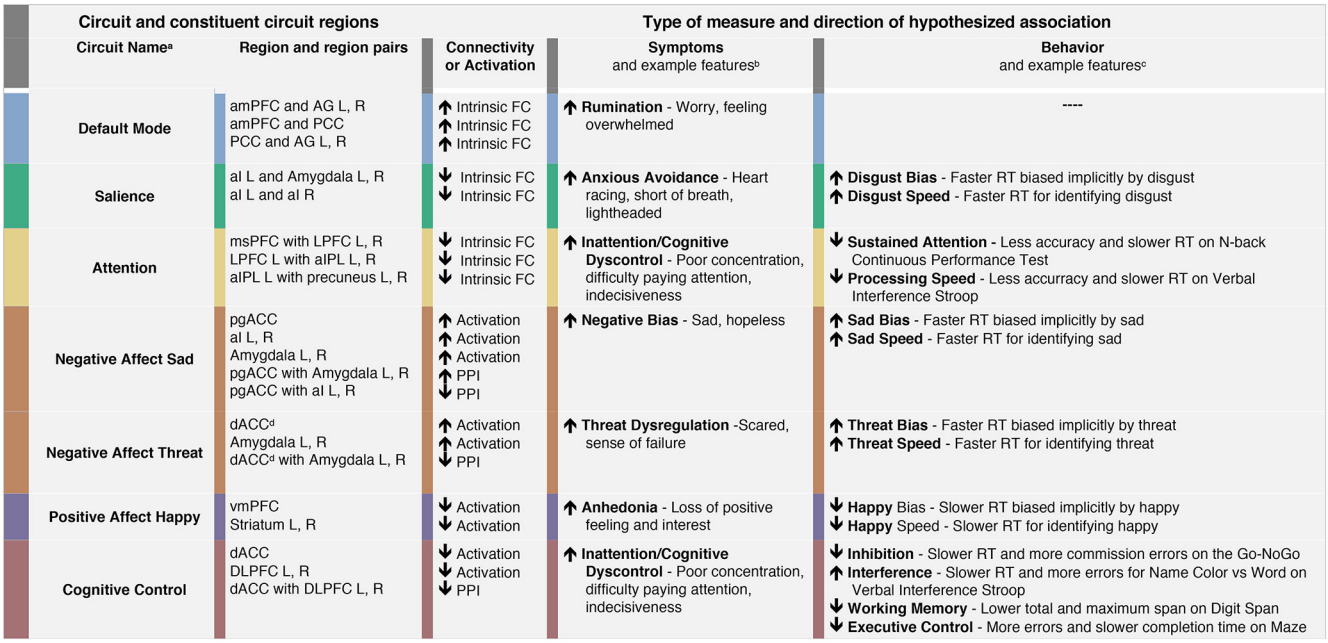

Circuit and constituent circuit regions			Type of measure and direction of hypothesized association	
Circuit Name[a]	**Region and region pairs**	**Connectivity or Activation**	**Symptoms** and example features[b]	**Behavior** and example features[c]
Default Mode	amPFC and AG L, R amPFC and PCC PCC and AG L, R	↑ Intrinsic FC ↑ Intrinsic FC ↑ Intrinsic FC	↑ **Rumination** - Worry, feeling overwhelmed	----
Salience	aI L and Amygdala L, R aI L and aI R	↓ Intrinsic FC ↓ Intrinsic FC	↑ **Anxious Avoidance** - Heart racing, short of breath, lightheaded	↑ **Disgust Bias** - Faster RT biased implicitly by disgust ↑ **Disgust Speed** - Faster RT for identifying disgust
Attention	msPFC with LPFC L, R LPFC L with aIPL L, R aIPL L with precuneus L, R	↓ Intrinsic FC ↓ Intrinsic FC ↓ Intrinsic FC	↑ **Inattention/Cognitive Dyscontrol** - Poor concentration, difficulty paying attention, indecisiveness	↓ **Sustained Attention** - Less accuracy and slower RT on N-back Continuous Performance Test ↓ **Processing Speed** - Less accurracy and slower RT on Verbal Interference Stroop
Negative Affect Sad	pgACC aI L, R Amygdala L, R pgACC with Amygdala L, R pgACC with aI L, R	↑ Activation ↑ Activation ↑ Activation ↑ PPI ↓ PPI	↑ **Negative Bias** - Sad, hopeless	↑ **Sad Bias** - Faster RT biased implicitly by sad ↑ **Sad Speed** - Faster RT for identifying sad
Negative Affect Threat	dACC[d] Amygdala L, R dACC[d] with Amygdala L, R	↑ Activation ↑ Activation ↓ PPI	↑ **Threat Dysregulation** -Scared, sense of failure	↑ **Threat Bias** - Faster RT biased implicitly by threat ↑ **Threat Speed** - Faster RT for identifying threat
Positive Affect Happy	vmPFC Striatum L, R	↓ Activation ↓ Activation	↑ **Anhedonia** - Loss of positive feeling and interest	↓ **Happy** Bias - Slower RT biased implicitly by happy ↓ **Happy** Speed - Slower RT for identifying happy
Cognitive Control	dACC DLPFC L, R dACC with DLPFC L, R	↓ Activation ↓ Activation ↓ PPI	↑ **Inattention/Cognitive Dyscontrol** - Poor concentration, difficulty paying attention, indecisiveness	↓ **Inhibition** - Slower RT and more commission errors on the Go-NoGo ↑ **Interference** - Slower RT and more errors for Name Color vs Word on Verbal Interference Stroop ↓ **Working Memory** - Lower total and maximum span on Digit Span ↓ **Executive Control** - More errors and slower completion time on Maze

Figure 1. Hypothesized directional relationships between circuit scores and phenotypes assessed by symptoms and behavior.

[a]For full details of Circuit Scores and Circuit Clinical Score, see Figures 2 and 3, Tables S4 and S5, and Methods S4; [b]For full details of composite measures of symptom phenotypes, see Tables S6 and S7 and Methods S6; [c]For full details of composite measures of behavior phenotypes, see Tables S8 and S9, and Methods S7. For details of daily function measures included in exploratory analyses, not shown in Figure 1, see Table S10 and Methods S8; [d]dACC was used for Negative Affect Conscious Threat and the sgACC was used for Negative Affect non-conscious threat.

Abbreviations: FC = Functional Connectivity; RT = Reaction Time.

Regional Abbreviations: ACC = Anterior Cingulate Cortex; AG = Angular Gyrus; aI = anterior Insula; aIPL = anterior Inferior Parietal Lobule; amPFC= anterior medial PreFrontal Cortex; dACC = dorsal Anterior Cingulate Cortex; DLPFC = Dorsolateral Prefrontal Cortex; L = Left; LPFC = Lateral Prefrontal Cortex; vmPFC = venromedial Prefrontal Cortex; msPFC = medial superior PreFrontal Cotex; pACC = pregenual ACC; PCC = Posterior Cingulate Cortex; PPI = PsychoPhysiological Interaction; R = Right.

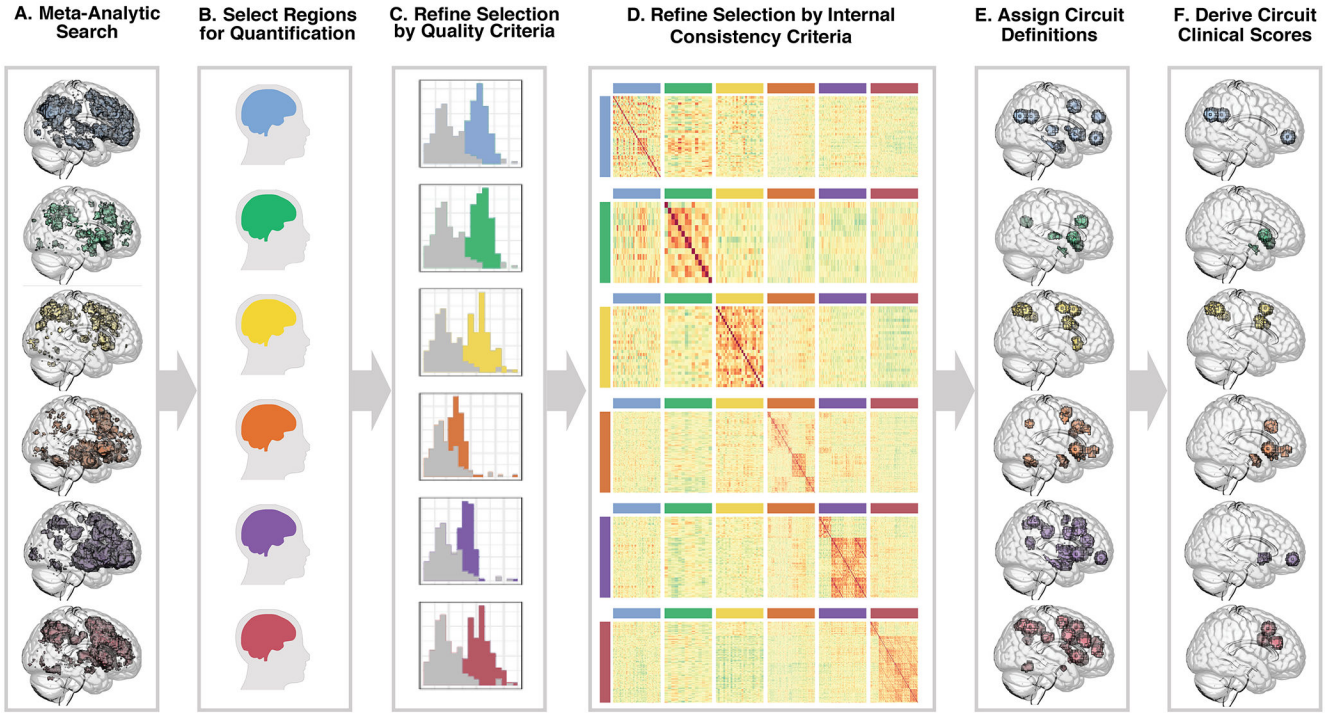

Figure 2. Quantifying circuits of interest.

First, we identified six target circuits of interest relevant to depression and anxiety and identified potential regions in these circuits using the meta-analytic database and search tool Neurosynth.org. From top to bottom, these circuits are default mode (blue), salience (green), attention (yellow), negative affect (orange), positive affect (purple), cognitive control (red) (A). To identify regions of interest (B) we considered the default mode, salience, and attention circuits to be task-free and the negative affect, positive affect, and cognitive control circuits to be task-evoked (details in Table S3). We refined our circuit features by first excluding regions based on low tSNR and low fit to gray matter (C). We evaluated internal consistency and excluded region pairs whose connectivity showed stronger associations with out-of-circuit region pairs than within-circuit region pairs in our healthy sample (E). From the resulting set of regions (E) we identified the subset implicated in hypothesized dysfunction and derived circuit clinical scores references to a healthy sample (F; details in Table S5).

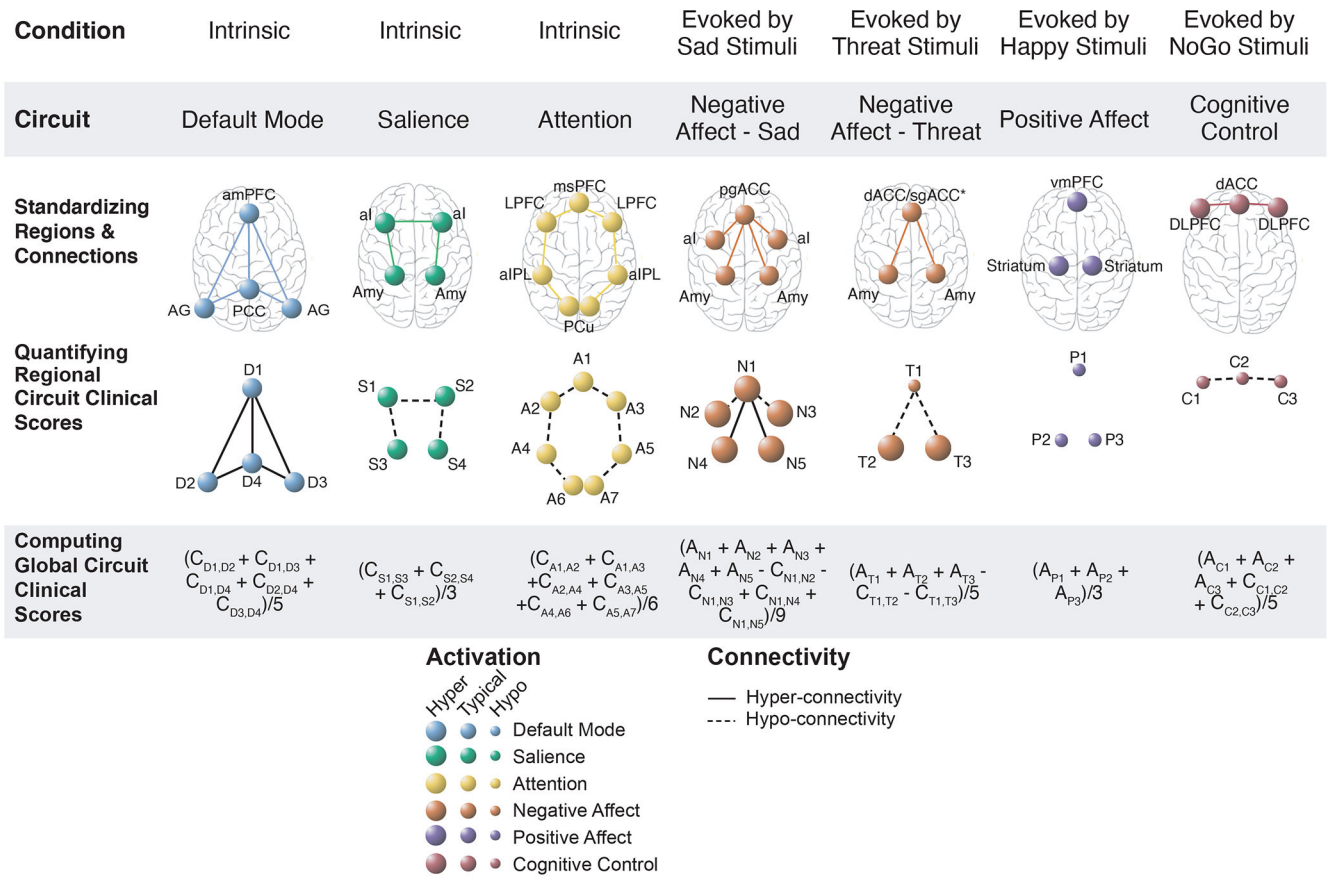

Figure 3. Quantifying global and regional circuit clinical scores.

An overview of the systematic process used to derive circuit clinical scores based on standardized definitions of the six circuits of interest and hypothesized dysfunction in these circuits in depression and anxiety. These circuits of interest were probed in both task-free and task-evoked conditions and were referred to as the default mode, salience, attention, negative affect, positive affect, and cognitive control circuits. A standardized procedure was used to identify and define constituent regions and region-to-region connectivity for each of these circuits (row 1). Activation and connectivity for each of these constituent regions was quantified at an individual subject level in clinical subjects and expressed in standardized units relative to a healthy reference sample mean such that the magnitude of resulting circuit clinical scores is interpretable relative to a healthy mean of 0 (row 2) These regional circuit clinical scores are assigned abbreviated labels (D1, D2, etc.) to facilitate subsequent computations. These constituent regions are assigned abbreviated labels (D1, D2, etc.) to facilitate subsequent computations. These regions may be visualized in to reflect the hypothesized direction of dysfunction in depression and anxiety (for example, connections between regions of the salience circuit care are illustrated by dashed lines to indicate hypothesized hypo-connectivity; row 2). Global circuit clinical scores were computed by averaging regional circuit inputs (row 3). The formulas used to generate these global circuit clinical scores are shown with the regional input labels and with regional activation inputs indicated by “A” and connectivity inputs indicated by “C”.

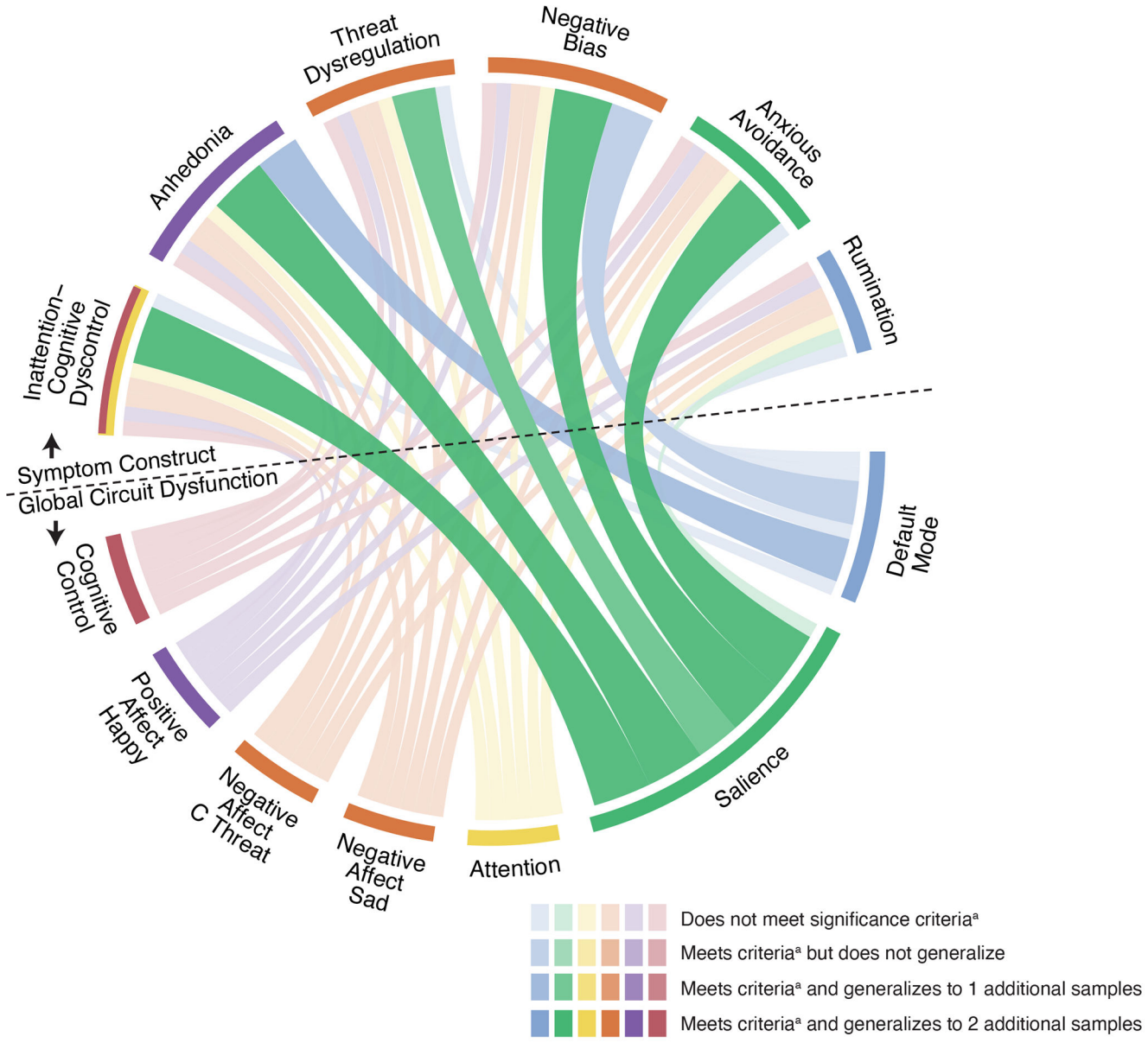

Figure 4. Visualization of the associations between global circuit clinical scores and phenotypes.

Observed relationships between global circuit clinical scores (bottom half; below the dotted line) and theoretically motivated symptom phenotypes (top half; above the dotted line). Significant relationships in the primary sample A are illustrated by thicker, darker lines, with the color of the ribbon representing the specific circuit involved and the thickness representing the magnitude of effect size (standardized regression coefficient values) and consistency of effects across samples. The color of the outermost ring of the circle's top half represents the corresponding hypothesized one-to-one mapping of circuit and phenotype (e.g. Default Mode network [blue] was hypothesized to map to the Rumination phenotype [blue] and the Salience circuit [green], to the Anxious Avoidance phenotype [green]). [a] Significant relationships are defined as those that survive the false discovery rate (FDR) threshold using the Benjamini-Hochberg procedure at q=0.05.

Abbreviations: C Threat = Conscious Threat.

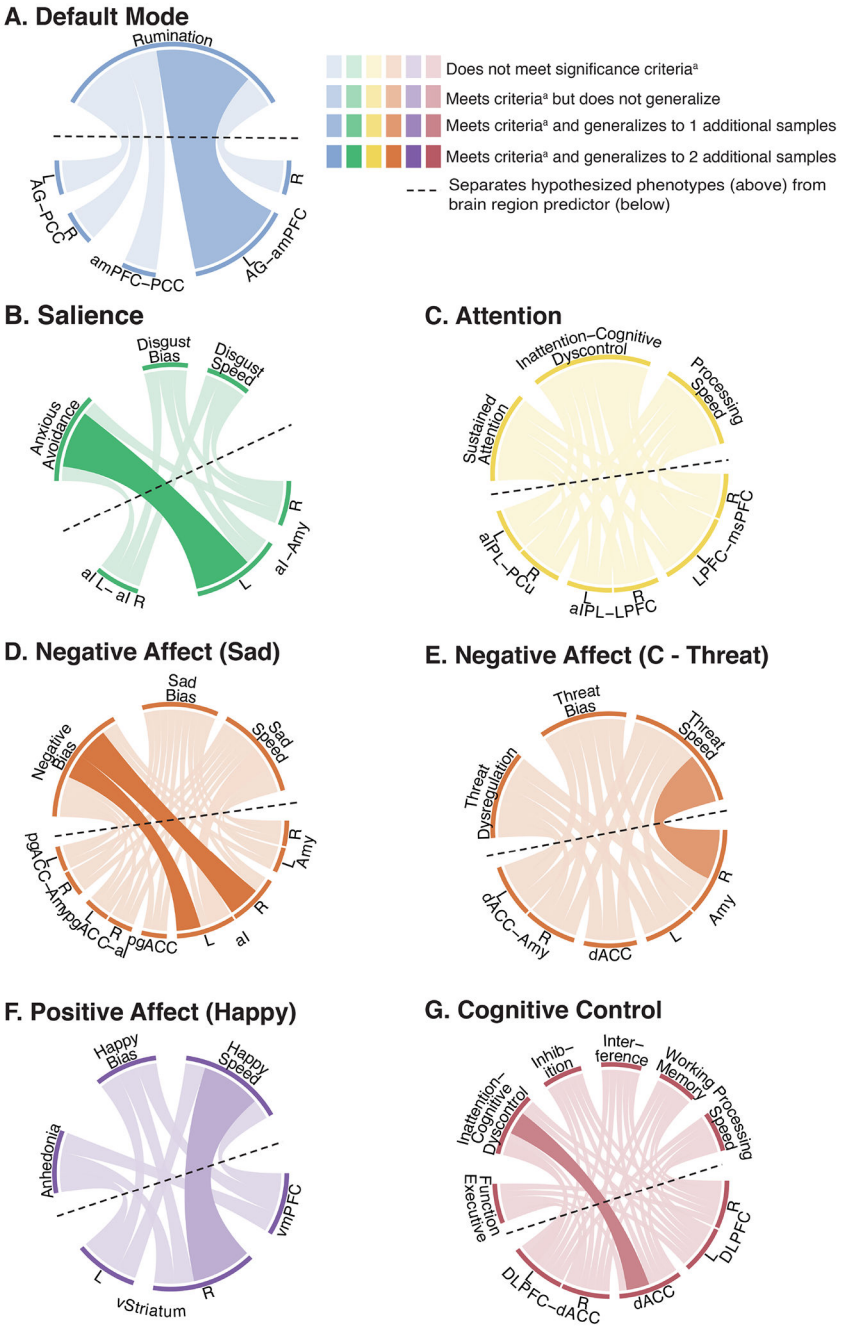

Figure 5. Visualization of the associations between regional circuit clinical scores and phenotypes.

The observed relationships between regional circuit clinical scores (bottom half of each circle; below the dotted line) and symptom and/or behavioral phenotypes (top half of each circle; above the dotted line), guided by our theoretical synthesis (A=default mode circuit, B=salience circuit, C=attention circuit, D=negative affect circuit elicited by sad, E=negative affect circuit elicited by threat, F=positive affect circuit, G=cognitive control circuit). Relationships in primary sample A (i.e., uncorrected $p<0.05$) are illustrated by thicker, darker lines, with the color representing the specific circuit involved and the thickness

representing the magnitude of effect size (standardized regression coefficient values) and consistency of effects across samples.

[a] Relationships observed at an uncorrected $p<0.05$.

Abbreviations: AG = Angular Gyrus; aI = anterior Insula; aIPL = anterior Inferior Parietal Lobule; amPFC = anterior medial Prefrontal Cortex; Amy = Amygdala; dACC = dorsal Anterior Cingulate Cortex; DLPFC = Dorsal Lateral Prefrontal cortex; L = Left; LPFC = Lateral Prefrontal Cortex; vmPFC = ventromedial Prefrontal Cortex; msPFC = medial superior Prefrontal Cortex; pgACC = pregenual Anterior Cingulate Cortex; PCC = Posterior Cingulate Cortex; PCu = Precuneus; R = Right; RT = Reaction Time; vStriatum = ventral Striatum.

Table 1.

Summary of Results for Relations between Circuit Score and Clinical Phenotypes

1. Results of models testing hypothesized predictions at the Global Circuit level										
				Primary Sample A			**Primary Sample B**		**Generalizability Sample**	
Global Circuit Clinical Score Predictor	**Dependent Variable**	**Domain**	**β (ES)**	**95% CI**	**t**	**p**	**β (ES)**	**Within CI**	**β (ES)**	**Within CI**
Salience	Anxious Avoidance	Symptoms	−0.26	[0.09, 0.44]	−2.98	0.008[a]	0.15	yes	0.11	yes
2. Results of models testing non-hypothesized predictions at the Global Circuit level										
				Primary Sample A			**Primary Sample B**		**Generalizability Sample**	
Global Circuit Clinical Score Predictor	**Dependent Variable**	**Domain**	**β (ES)**	**95% CI**	**t**	**p**	**β (ES)**	**Within CI**	**β (ES)**	**Within CI**
Default Mode	Negative Bias	Symptoms	−0.25	[−0.40, −0.07]	−2.59	0.009[a]	0.14		−0.05	
Default Mode	Anhedonia	Symptoms	−0.24	[−0.40, −0.06]	−2.50	0.010[a]	0.05		−0.09	yes
Salience	Inattention/Cognitive Dyscontrol	Symptoms	−0.19	[0.01, 0.35]	−2.03	0.031[a]	0.15	yes	0.17	yes
Salience	Negative Bias	Symptoms	−0.26	[0.07, 0.45]	−2.78	0.008[a]	0.16	yes	0.17	yes
Salience	Threat Dysregulation	Symptoms	−0.23	[0.06, 0.39]	−2.43	0.011[a]	0.16	yes	0.05	
Salience	Anhedonia	Symptoms	−0.27	[0.06, 0.47]	−2.87	0.006[a]	0.10	yes	0.09	yes
Salience	Satisfaction with life	Function	−0.24	[−0.42, −0.06]	−2.58	0.009[a]	−0.09	yes	−0.05	
3. Results of models testing hypothesized predictions at the Regional Circuit level										
				Primary Sample A			**Primary Sample B**		**Generalizability Sample**	
Regional Circuit Predictor	**Dependent Variable**	**Domain**	**β (ES)**	**95% CI**	**t**	**p**	**β (ES)**	**Within CI**	**β (ES)**	**Within CI**
Default Mode: L AG-amPFC connectivity	Rumination	Symptoms	−0.21	[−0.38, −0.01]	−2.39	0.029	−0.07	yes	0.04	
Salience: L AI –L Amy connectivity	Anxious Avoidance	Symptoms	−0.26	[−0.42, −0.11]	−2.96	0.006[a]	−0.23	yes	−0.17	yes
Negative Affect (Sad): L AI activation	Negative Bias	Symptoms	−0.20	[−0.37, −0.01]	−2.15	0.027	−0.17	yes	−0.06	yes
Negative Affect (Sad): R AI activation	Negative Bias	Symptoms	−0.21	[−0.38, −0.01]	−2.15	0.029	−0.23	yes	−0.14	yes
Negative Affect (C-Threat): R Amy activation	Threat Speed	Behavior	−0.19	[−0.34, −0.04]	−2.15	0.047	−0.18	yes	−0.04	
Positive Affect (Happy): R VS activation	Happy Speed	Behavior	−0.20	[−0.34, −0.06]	−2.28	0.045	−0.06	yes	−0.05	
Cognitive Control: ACC activation	Inattention/Cognitive Dyscontrol	Symptoms	−0.26	[−0.41, −0.06]	−2.69	0.013	0.08		−0.16	yes

1. Results of models testing hypothesized predictions at the Global Circuit level										
			Primary Sample A				Primary Sample B		Generalizability Sample	
Global Circuit Clinical Score Predictor	**Dependent Variable**	**Domain**	**β (ES)**	**95% CI**	**t**	**p**	**β (ES)**	**Within CI**	**β (ES)**	**Within CI**
4. Results of models testing non-hypothesized predictions at the Regional Circuit level										
			Primary Sample A				Primary Sample B		Generalizability Sample	
Regional Circuit Predictor	**Dependent Variable**	**Domain**	**β (ES)**	**95% CI**	**t**	**p**	**β (ES)**	**Within CI**	**β (ES)**	**Within CI**
Default Mode: R AG- amPFC connectivity	Negativity Bias	Symptoms	−0.19	[−0.37, −0.02]	−2.01	0.049	0.04		0.00	
Salience: L AI–R AI connectivity	Negativity Bias	Symptoms	−0.30	[−0.50, −0.10]	−3.28	0.002[a]	0.07		−0.29	yes
Salience: L AI–R AI connectivity	Threat Dysregulation	Symptoms	−0.27	[−0.51, −0.01]	−2.95	0.005[a]	−0.03	yes	−0.08	yes
Salience: L AI–R AI connectivity	Anhedonia	Symptoms	−0.33	[−0.52, −0.12]	−3.57	0.001[a]	0.01		−0.25	yes
Salience: L AI–L Amy connectivity	Satisfaction with life	Function	0.18	[0.01, 0.37]	1.98	0.049	0.23	yes	−0.12	
Salience: L AI–R AI connectivity	Satisfaction with life	Function	0.24	[0.03, 0.43]	2.59	0.015[a]	0.01		0.21	yes

1. Results of models testing hypothesized associations of Global Circuit Clinical Scores as Predictors and Phenotypes as Dependent Variables.

[a]indicates results meeting family-wise FDR correction of 0.05 in Primary Sample A and 'yes' indicates instances where the relationship generalizes to Primary Sample B and/or Generalizability samples (i.e., the standardized beta coefficient, β, falls within the 95% interval of the primary A sample).

Predictor and Dependent Variable are coded in the same color rerflectinig the reflect the presence of a *hypothesized* association (e.g. Salience: Circuit Clinical Score – Anxious Avoidance)

2. Results of models testing non-hypothesized associations of Global Circuit Clinical Scores as Predictors and Phenotypes as Dependent Variables. [a]indicates results meeting family-wise FDR correction of 0.05 in Primary Sample A and 'yes' indicates instances where the relationship generalizes to Primary Sample B and/or Generalizability samples. Predictor and Dependent Variable are coded in different color rerflectinig a *non-hypothesized* association (e.g. Default Mode: Global Circuit Clinical Score – Negativity Bias).

3. Results of models testing hypothesized associations of Regional Circuit Clinical Scores as Predictors and Phenotypes as Dependent Variables. [a]indicates results meeting family-wise FDR correction of 0.10 in the Primary Sample A and 'yes' indicates instances where the relationship generalizes to Primary Sample B and/or Generalizability samples.

4. Results of models testing non-hypothesized associations of Regional Circuit Clinical Scores as Predictors and Phenotypes as Dependent Variables. [a]indicates results meeting family-wise FDR correction of 0.10 in the Primary Sample A and 'yes' indicates instances where the relationship generalizes to Primary Sample B and/or Generalizability samples.

Abbreviations:

β = Standardized beta coefficients; CI = Confidence Interval for the effect size represented by the value of β; ES = standardized effect size represented by the value of β, standardized beta coefficient for contribution of circuit dysfunction predictors to clinical phenotype.

Regional Abbreviations:

ACC = Anterior Cingulate Cortex; AG = Angular Gyrus; AI = Anterior Insula; amPFC = anterior medial PreFrontal Cortex; Amy = Amygdala; C = Consicous; L= Left; R= Right; VS = ventral Striatum.

KEY RESOURCES TABLE

Resource Type	Specific Reagent or Resource	Source or Reference	Identifiers	Additional Information
Add additional rows as needed for each resource type	Include species and sex when applicable.	Include name of manufacturer, company, repository, individual, or research lab. Include PMID or DOI for references; use “this paper” if new.	Include catalog numbers, stock numbers, database IDs or accession numbers, and/or RRIDs. RRIDs are highly encouraged; search for RRIDs at https://scicrunch.org/resources.	Include any additional information or notes if necessary.
Antibody	NA			
Bacterial or Viral Strain	NA			
Biological Sample	NA			
Cell Line	NA			
Chemical Compound, Drug	NA			
Commercial Assay Or Kit	NA			
Deposited Data; Public Database	NDA	NIMH Data Archive	https://nda.nih.gov/, Collection C2100	
Organism/Strain	NA			
Sequence-Based Reagent	NA		N/A	
Software; Algorithm	MATLAB-2014b	MathWorks	RRID:SCR_001622	
Software; Algorithm	Singularity 3.2.1	https://github.com/sylabs/singularity/releases/tag/v3.2.1	N/A	
Software; Algorithm	FSL 5.0	Analysis Group, FMRIB, Oxford, UK	RRID:SCR_002823	
Software; Algorithm	SPM 8	Wellcome Centre for Human Neuroimaging, UCL	RRID:SCR_007037	
Software; Algorithm	AFNI 19.0.07	NIMH Scientific and Statistical Computing Core	RRID:SCR_005927	